RSC Advances

ROYAL SOCIETY OF CHEMISTRY

www.rsc.org/advances

Graphical abstract

A newly synthesized giant mesoporous silica particle has been used for arsenate and chromate adsorption studies.

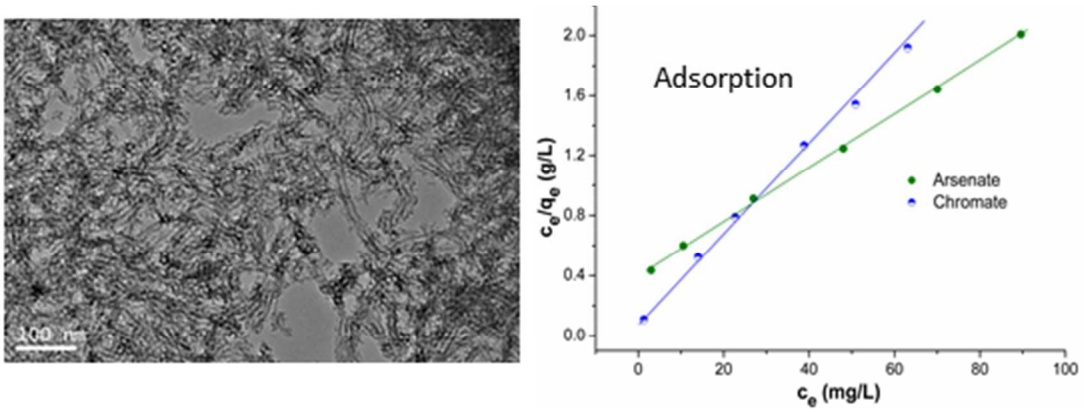

Journal Name

RSCPublishing

ARTICLE

Mesoporous silica-giant particle with slit pore arrangement as adsorbent for heavy metal oxyanions from aqueous medium

Cite this: DOI: 10.1039/x0xx00000x

Received 00th January 2012,
Accepted 00th January 2012

DOI: 10.1039/x0xx00000x

www.rsc.org/

Seenu Ravi,[a] Roshith Roshan,[a] Jose Tharun,[a] Dae-Won park,[a] Ho-Hwan Chun,[b] Hyun Park [b] and Manickam Selvaraj,*[a]

Incessant formation of chain like IBN-4 mesoporous silica (ICMS-N) with long channels running along the length of hexagonal rods have been directly synthesized by cocondensation of 3-aminopropyltriethoxysilane (APTES) and tetraethylorthosilicate as silica source in presence of Pluronic P123 and Fluorocarbon (FC-4) surfactants as structure directing agents. The newly synthesized materials were successfully characterized through SAXS, N_2-physisorption, FT-IR, XPS, ^{29}Si NMR, TEM, SEM and elemental analysis. The TEM images evidenced the chain like morphologies and SEM studies showed that the synthesized ICMS-N particles possess >10 μm length. Moreover the so formed material was tested for the removal of oxyanions such as arsenate and chromate, is exhibited maximum adsorption capacity of 55 and 35 mg/g of ICMS-N15, respectively. The formation of quaternary species of amine on the surface of the ICMS-N enhanced the adsorption capacity towards arsenate and chromate under acidic pH and the adsorption isotherm fits with Langmuir monolayer adsorption. Naturally existing anions such as nitrate, sulfate, phosphate and chlorides with 1×10^{-2} M have no significant effect on the adsorption of heavy metal ions. The reusability tests have also been carried out.

Introduction

Pollutants exist in a variety of forms in contaminated water and among which arsenic and chromium ion pollution are detrimental to bio life. Arsenic in various sample matrixes causes a multitude of serious health problems and their presence in drinking water in less developed countries has become one of the biggest environmental problems of the century. Similarly, the commonly existing Cr(VI) and Cr(III) in surface and ground water are arising from anthropogenic and geological processes. [1-2]. The former (CrVI) has been recognized as a serious environmental problem due to its toxicity to living organisms and potential carcinogenicity to humans. [3], Thus, creating arsenic and chromium free environment has become one of the most important tasks when evaluating their toxic effects. Over the past few decades, methods for reducing environmental contaminants have included adsorption techniques, precipitation, electrochemical reduction, membrane filtration and ion exchange [4-9]. Among these techniques, the adsorption is preferred owing to its simplicity and economic feasibility. Recently, porous particles possessing high textural properties have substantial growth in adsorption technique including mesoporous silicas [10-11], activate carbon [12-13], mesoporous magnetic particles [14-15], bio-sorbents [16-17] and hybrid polymeric adsorbent [18] have been used for various environmental contaminants. Of particular interest are mesoporous silica materials, which have been used in challenging applications such as catalysis, drug delivery and energy storage [19-21].

Demand for highly designed mesoporous silica materials has been increased in the adsorption studies owing to their interesting physical properties such as high surface area, pore volume and pore sizes. These structural regularities have been appeared either by the effect of structure directing agents or synergistic role of surfactants and organosilanes. For example

combination of co-surfactants with non-ionic surfactants can cause formation of astonishing materials with various structural/geometrical arrangement and phenomenal textural properties [22]. Similarly cationic surfactants also produced variety of new morphological silicas owing to their reorganization effect with nonionic surfactants [23]. However synthesizing morphologically controlled large pore amino functionalized 2D mesoporous silicas are probably the difficult synthesis approach in presence of nonionic surfactant [24]. Nevertheless the direct controlled addition of organosilane into the SBA-15 mesoporous silica results nanostructured hexagonal platelet morphology [25]. By rationalizing the above context it would be possible to obtain a different morphological mesoporous silica when the amine precursor has used in presence of binary surfactants medium. Similar discoveries of nanomaterials have found useful in number of applications [26-28]. Owing to the higher diffusion and external pore arrangement, 2D mesoporous silicas exhibit appreciable activity during adsorption process [29-30]. Recently, there has been significant push to synthesis mesoporous silica adsorbents because of their promising industrial and technological applications. The basic strategy to trap toxic anions by silica adsorbent is to immobilize surface amino groups or metal-chelated ligands on the mesoporous surface, implying high affinity and selectivity [31-40]. To the best of our knowledge, no reports have been made on the formation of chain like open slit pore mesoporous silica through direct functionalization of amine precursor.

In this study, we report a morphologically controlled chain like slit pore IBN-4 mesoporous silica, synthesized directly from the cocondensation of tetraethylorthosilicate and 3-aminopropyltriethoxysilane (APTES) in presence of Pluronic P123 and FC-4 binary surfactants as structure directing agents under weak acidic medium. Their efficacies for the adsorption of arsenate and chromate ions were studied for the first time.

Result and discussion

Influence of 3-aminopropyltriethoxysilane on ICMS-N formation

When the nonionic P123 dispersed with FC-4 surfactant micelles produced irregular rod like silica particles (IBN-4) with p6m pore geometry [22]. To animate this IBN-4, a primary amine content APTES with different mole ratios has been functionalized through a direct method, based on our previous report [28]. The obtained materials has deformed its outer morphology from small rode like to continuous long channeled arrangement, is displayed in the TEM image (Fig. 1), characteristic to 2D hexagonal mesoporous silica. Since the material infused with two different mole ratios of amine precursor such as 0.5 and 1.5 and they were named as ICMS-N5 and ICMS-N15, respectively.

The 2D hexagonal morphology of ICMS-N materials also evidenced by the SAXS patterns Fig. 2, shows three well resolved peaks for ICMS-N5, which can be indexed to (100), (110) and (200) reflections surmised mesostructures of hexagonal space group p6m. In the case of ICMS-N15 the higher order diffraction peaks were too weak due to greater incorporation of APTES into the framework. However, the intense diffraction peak at q=0.57 nm^{-1} and 0.58 nm^{-1} of ICMS-N5 and ICMS-N15 is corresponding to 2θ= 0.83 and 0.85, respectively, characteristic of hexagonal framework. The difference in d spacing value of IBN-4 [31] and ICMS-N materials also infers the structural changes as noted in the Table 1.

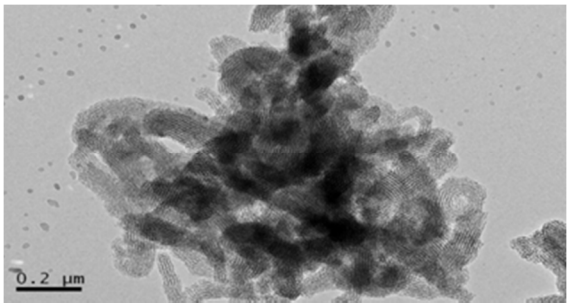

Fig. 1 TEM image of ICMS-N particles

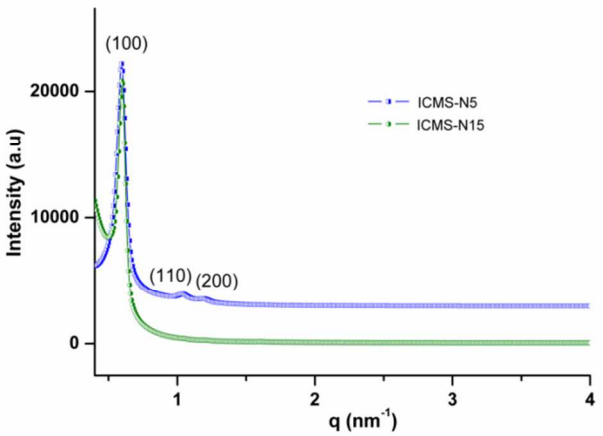

Fig. 2 SAXS patterns of ICMS-N5 and ICMS-N15.

The mesoporosity of the samples were determined using nitrogen sorption analysis. The N_2 adsorption desorption isotherm of samples in Fig. 3, exhibited type IV isotherm with H_3 hysteresis loop, indicating that this sample has a mesoporous structure with open pore slit-shaped framework[41]. But the pristine IBN-4 shown type IV isotherm with H1 hysteresis loop suggested mesoporosity of hexagonal morphology with cylindrical pore network [28]. The convergence at 0.6 of adsorption and immediate desorption (1.0) implied that the

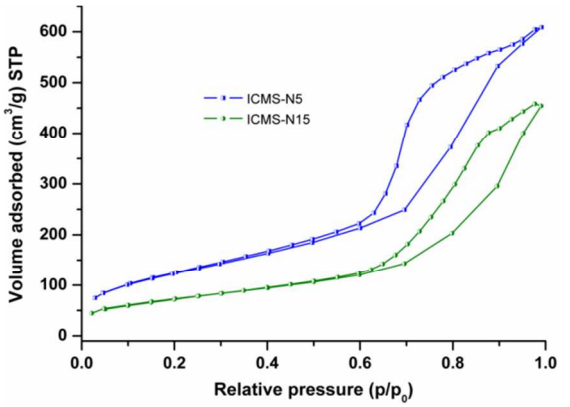

Fig. 3 N_2 adsorption–desorption isotherms of ICMS-N5 and ICMS-N15

materials possess slit type large pore sizes with narrow distributions. This was confirmed by the pore size distributions calculated using a BJH (Barrett, Joyner and Halenda) method from the adsorption branches, which exhibited narrow pore distributions with maxima between 10 and 11 nm. The surface area of ICMS-N5 and ICMS-N15 were 368 and 262 m^2/g, respectively, and all the textural properties were summarized in Table 1.

Table 1 Textural properties of APTES functionalized IBN-4

Materials	d (nm)	S_{BET} [a] (m^2/g)	D_p [a] (nm)	V_p [a] (cm^3/g)	N [b] mmol/g
IBN–4	6.93	512	4.3	0.9	0
ICMS-N5	11.01	368	6.2	0.83	0.4
ICMS-N15	10.72	262	7.2	0.71	1.47

d_{100}- spacing value, S_{BET}-surface area, D_p-pore diameter, V_p-pore volume.[ICMS-N5 and ICMS-N15 denotes APTES functionalized chain-like IBN-4 with 5 & 15 mole percentages respectively]. [a] These values were obtained from N_2 physisorption studies. [b] Calculated from elemental analysis.

The presence of organic groups in ICMS-N5 and ICMS-N15 materials was corroborated by the FT–IR spectroscopic analysis as displayed in Fig. 4. The propyl groups attached to the silicon framework were confirmed by the $–CH_2–$ stretching bands present between 2975-2925 cm^{-1}, suggesting the attachment of organic moieties on the silica surface. The band at 1448 cm^{-1} was assigned to the $–CH_2–$ symmetric bending mode vibration. A large broad band between 3600-3010 cm^{-1} was attributed to the O–H stretching mode of silanol groups. The absorption bands at 1096 and 803 cm^{-1} were assigned to Si–O–Si and Si–O stretching vibrations, respectively. Characteristic bands at 958 cm^{-1} were assigned to Si–OH stretching vibrations.

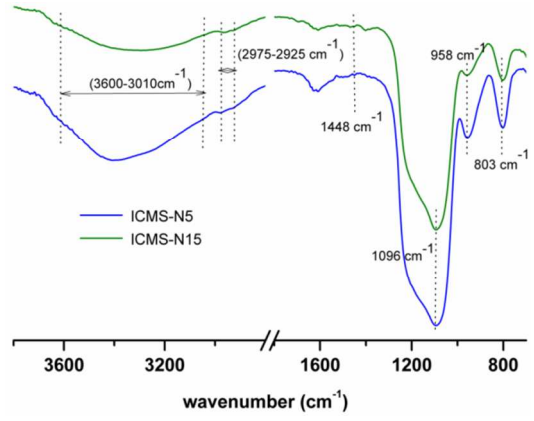

Fig. 4 FT-IR spectra of ICMS-N5 and ICMS-N15

The SEM image (Fig. 5) revealed that the synthesized ICMS-N samples from the cocondensation reaction of TEOS and APTES in presence of P123 and FC-4 surfactant under weak acidic medium have long rod like particles when the set mole ratio of APTES is 5%. Once it increases to 15%, the aggregated rod like particles dispersed into long channeled giant particles. This effect was clearly observed from the TEM image is as shown in Fig. 6. Therefore the amount of APTES in IBN-4 can control the formation of long rod like particles. The brighter part of SEM image is appeared due to the surface charging effect. The TEM analyses indicated that the materials have highly ordered mesoporous structures with 2D hexagonal arrangement (Fig. 6). The TEM image also clearly showed that materials have long pore channels similar to SBA-15 materials. Besides the particle width is very less when compared to pristine IBN-4 materials [22]. The reduction in thickness as well as diameter arises due to the repulsive interaction of positively charged APTES to the fluorocarbon surfactant, also consequences the slit pore arrangement. The range of open pore network and the particle length was goosed up to the long range of >10 μm respective to the amount of amine precursor. This can also be explained, upon increasing the concentration of APTES, the degree of interconnection of small rod like particles has substantially increased. Materials prepared at the weak acidic solution exhibits the largest degree of such interaction [42]. This skeletal long channeled formation is only possible with APTES and no such chain-like arrangements formed when the functionalization of other amine precursors such as diamine and triamine source into IBN-4 silica, as shown in Fig. S1. Moreover, after the structural transformation the presence of amine group on the surface of ICMS-N15 was confirmed from the XPS analysis is shown in Fig. S2. The ordered open pore entrances ICMS was obtained up to 15 mol% of APTES and further incorporation of APTES results block spots on the pore entrances owing particle disorderliness Fig. S3.

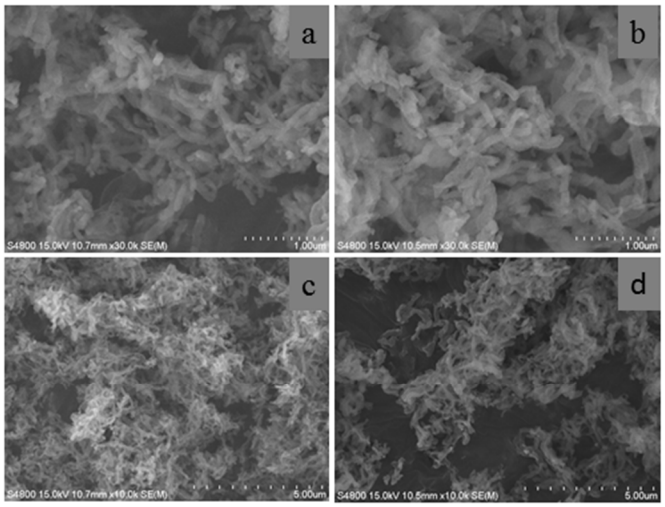

Fig. 5 SEM images of ICMS-N5 (a & c) and ICMS-N15 (b & d)

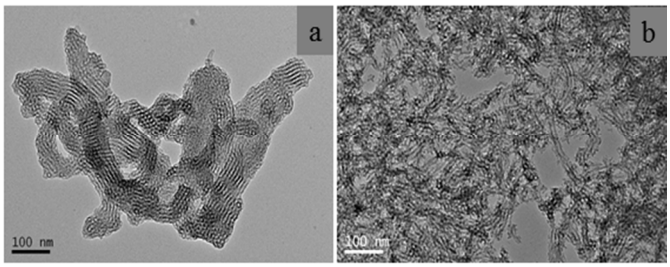

Fig. 6 TEM images of ICMS-N5 (a) and ICMS-N15 (b)

The extent of the functionalization of the primary amine precursor moiety into the IBN-4 was further identified through the ^{29}Si-CP/MAS NMR spectra (Fig. 7). The spectrum of the

ICMS shown three peaks at −110, −100 and −93 ppm which are attributed to silicon in the siloxane binding environment without a hydroxyl group [$(SiO)_4Si$], the isolated silanol group [$(SiO)_3Si–OH$] and to the geminal silanol groups [$SiO]_2Si–(OH)_2$] of the silica support which are denoted as Q_4, Q_3 and

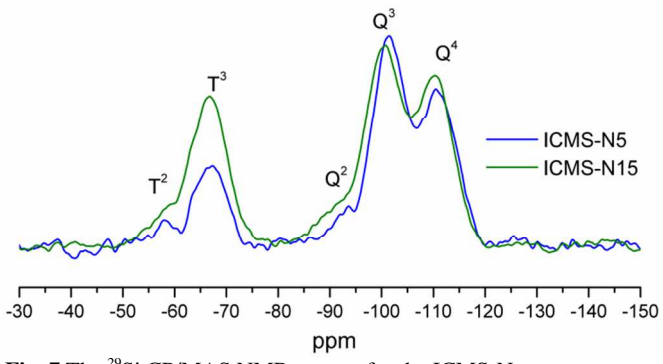

Fig. 7 The ^{29}Si CP/MAS NMR spectra for the ICMS-N

Q_2, respectively.[28] In addition to these peaks, two additional peaks can be observed at −58 and −67 ppm, which correspond to two different environments for the siloxane groups i.e., the amine functionalized layers and these are represented as T2 and T3 respectively. The quantitative determinations of amine in the ICMS-N materials were done by elemental analysis. The corresponding values are given in Table 1.

Adsorption studies

Adsorption isotherm

The equilibrium adsorption isotherm was used to understand the mechanism of heavy metal ion interactions in the adsorption systems. In order to conduct adsorption studies, a mixture of ICMS-N15 in aqueous solutions containing known amounts of arsenate were prepared. The mixture was stirred until equilibrium was reached. Similarly, chromate studies were also done. The adsorption isotherms of arsenate and chromate at room temperature are shown in Fig. 8a.

The equilibrium adsorption capacity (q_e) increases with the initial concentration of adsorbates (C_0). The Langmuir isotherms model gives the adsorption capacity and also gives insight about surface properties and adsorbent/adsorbate affinity constants. Assuming monolayer adsorption without any interaction between adsorbed molecules, the Langmuir isotherm model can be expressed as [43],

$$\frac{c_e}{q_e} = \frac{1}{bq_m} + \frac{c_e}{q_m}$$

where C_e is the equilibrium concentration of adsorbates in the aliquots (mg L^{-1}), q_e defines the amount of adsorbate adsorbed on the unit amount of the adsorbent at equilibrium (mg g^{-1}), q_m denotes the maximum adsorption capacity of adsorbent (mg g^{-1}), and b is the affinity of binding sites or the Langmuir constant (L mg^{-1}).

The arsenate and chromate adsorption isotherms of ICMS-N15 exhibit typical Langmuir behavior like other amino functionalized adsorbents [44], suggesting monolayer adsorption on independent binding sites (Fig. 8b). This monolayer adsorption also supported by the stoichiometric ratios of amine towards arsenate and chromate are 0.26 and 0.19, respectively. This was calculated from the maximum adsorption capacity (qm) of arsenate and chromate are 55 and 35 mg (Table 2), respectively, to the mole value of amine in ICMS-N15. A comparative study has been done with the previously reported hexagonal mesoporous silica materials (Table S1). The calculated Langmuir constant (b) is summarized in Table 2. Moreover the correlation coefficient factor (R^2) of the Langmuir adsorption isotherm for both arsenate and chromate is ≥ 0.99.

Effect of pH and time

The adsorption capacity of an adsorbent for anionic metal species depends on the chemical and physical properties of the adsorbent and pH conditions of the sample matrix. Anionic arsenate species can distribute into several ionic species spontaneously under various pH conditions [40]. Chromate ions

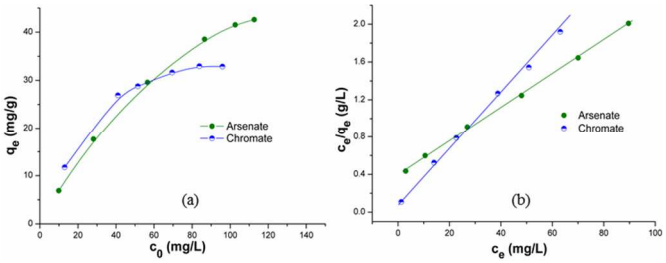

Fig. 8 (a) Adsorption isotherm, (b) Langmuir adsorption isotherm of arsenate and chromate over ICMS-N15

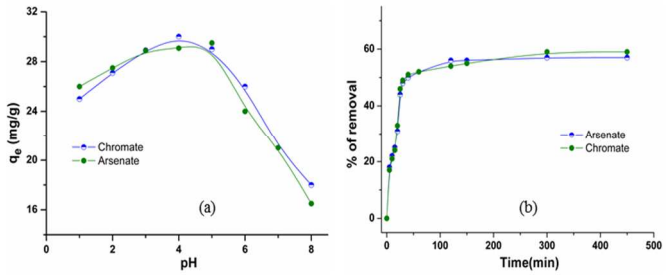

Fig. 9 (a) Effect of pH, (b) Effect of time on the adsorption of arsenate and chromate by ICMS-N15 at 50 ppm solution

Table 2 Langmuir adsorption isotherm plot values

	q_m (mg/g)	b (L/mg)	R^2
As- ICMS-N15	54.64	0.046	0.998
Cr- ICMS-N15	34.60	0.272	0.990

Where, q_m- maximum adsorption capacity, b- Langmuir constant, R^2-correlation coefficient.

can act as poly acids and can also be distributed into several ionic species under strong pH conditions [45]. The effect of pH on arsenate and chromate adsorption of ICMS-N15 with 50 ppm of stock solution was determined and their corresponding removal efficiencies are shown in Fig. 9a. An examination of ICMS-N15 treated over a long time in a wide range of pH conditions revealed the optimum range of pH to attain

maximum adsorption for chromate and arsenate is 3-4 and 4-5 respectively. At low pH conditions (< 3) protonation of the surface sites diminishes the number of negatively charged sites while upsurges the number of positively charged sites. The formation of quaternized amine ($NH_3^+Cl^-$) under the acidic conditions enhances the adsorption activity of ICMS-N. Accordingly, the adsorption percentage is higher under acidic conditions (pH < 6) than under basic conditions. With increasing pH from 2.0 to 8.0, the As (V) species were changed from H_3AsO_4 to AsO_4^{3-} via $H_2AsO_4^-$ and $HAsO_4^{2-}$ [46]. Though the adsorbates are anionic species at basic conditions, but amine groups are inactive with increasing -OH content in solution. Similar concept is applicable for chromate ions.

Efforts toward the development of mesostructured silica for faster adsorption of arsenate and chromate have been mostly concerned with the incorporation of amine groups, because nitrogen possesses a strong affinity for arsenic and chromium. The removal efficiency of ICMS-N15 showed that within 50 min the adsorption capacity reached about 50% in both cases, and took a further 30-50 min to reach the maximum capacity of 58% for chromate and 56% for arsenate at 50ppm solution (Fig. 9b).

Effect of naturally existing ions

Naturally existing other ions in aqueous systems may affect the adsorbent sites by entering into the pore wall prior to the targeted anions, which will adversely affect the adsorption reaction. In our study, the effect of naturally existing common anions (NEA) such as NO_3^-, Cl^-, PO_4^{3-}, and SO_4^{2-} on adsorbent properties was studied (Fig. S4). The effect of these anions follows in the order $PO_4^{3-}>SO_4^{2-}>Cl^->NO_3^-$, which affects the adsorption of arsenate and chromate. To analyze their effect on adsorption process, similar metal (sodium) salts has been chosen and tested with different ionic strength. As observed from the results, with increasing concentration of these ions decreased the adsorption of arsenate and chromate. The maximum influence of NEAs was about 51 and 55% for the former and latter respectively, when the NEA concentration is reaches to 0.005 M. This has also to be explained by Guoy Chapman model suggested that when solid charged adsorbent comes into contact with adsorbate species in solution, the latter is surrounded by an electrically diffused double layer, the thickness of which is significantly expanded by the presence of salts. This expansion inhibits the adsorbent particles and heavy metal anions species from approaching each other more closely, and through decreased electrostatic attraction, leads to the decreased uptake of heavy metal anions on the adsorption sites at employed conditions [49]. This indicates that at lower concentration (0.001M) of other ions does not have significant influence on the adsorption of arsenate and chromate. Moreover, the targeted oxyanions act as strong binding ligands towards amino groups binded on chain-like mesoporous silica.

Adsorbent regeneration

The recycling test of adsorbent explains the robustness and economic feasibility. Since the adsorption process is highly dependent on the solution pH, the adsorbent can be regenerated by altering the pH. The adsorptions of oxyanions were inefficient or at a minimal above pH 8, hence the ICMS-N15 regeneration could be done using NaOH solution of pH (10-11). But mesoporous silicas (Si-O-Si) bonds are susceptible to break with sodium hydroxides ions at higher concentration (pH > 10). Alternatively we have used NH_4OH and NH_4Cl (1: 2) solution (pH9-10) to desorb the oxyanions. This buffer can maintain the solution pH, meanwhile the excess chloride can restrict the interaction of desorbed chromate and arsenate ions to the amino moiety of ICMS-N15. Subsequently, we have found about 93% arsenate and 95% of chromate were desorbed from the catalyst. The generated catalyst produced sufficient results for the next three cycles as shown in Fig 10.

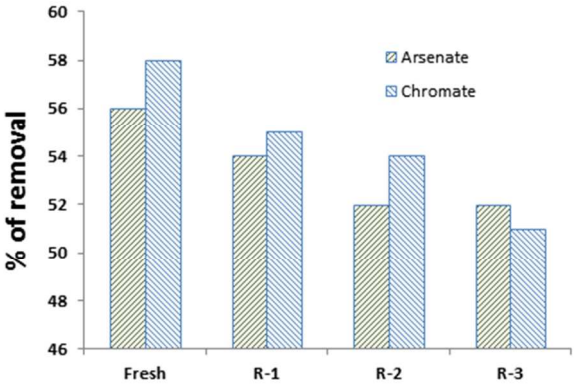

Fig. 10 Adsorbent regeneration (in each cycle 100 ml of 50 ppm heavy metal solution was treated with 100 mg of ICMS-N15)

Conclusion

The giant chain like formation of mesoporous silica with long channeled pore system was synthesized through the direct functionalization of APTES into the IBN-4 synthesis medium (ICMS-N). It was found that the synthesized ICMS-N particle length was increased upon increasing the APTES mole percentage. Moreover the ordered pore network even after the functionalization was achieved by controlling the mole ratio of amine precursor. The formation pathway of long channeled morphology of ICMS-N with open slit pore arrangement could be explained by various prospects such as, sticky end mechanism, protonation factor of amine groups and repulsive interaction of fluorocarbon surfactants. In addition, this newly synthesized material exhibited higher adsorption capacity towards chromate and arsenate oxyanions and their appreciable stoichiometric ratios explained their efficacies on adsorption studies. The protonation of amine at acid medium is thought to be the reason for their higher activity in adsorption mechanism. The average concentration of NEAs 1×10^{-2} M did not have significant effect on the adsorption reaction compared with the targeted ions.

Experiments

Material Synthesis

IBN-4 was synthesized as per the reported article [22] and the chemicals used to synthesize IBN-4 are Poly-block copolymer Pluronic 123 (P123), Fluorocarbon (FC-4), Tetraethyl Orthosilicate (TEOS), Hydrochloric acid and Water. Here we have done the direct functionalization of 3-aminopropyl trimethoxysilane (APTES) into IBN-4 mesoporous silica (ICMS-N). In this synthesis, the surfactants P123 and FC-4 were dissolved in acidified water and stirred at 30 °C until a clear solution were formed. Subsequently, TEOS (1-X mole)

mole was added drop wise into the synthetic solution until the prehydrolysis time followed by the addition of X mole of APTES (X= 0.05 and 0.15 mole), and the reaction was continued for 24–36 h at 30 °C. The reaction mixture was then transferred into a Teflon-lined autoclave and heated in an oven at 100 °C for 24–36 h. The resulting gel solution were filtered and dried in a vacuum oven at 60 °C for 6 h. ICMS-N5 and ICMS-N15 (corresponding to solutions with 5 and 15% mole ratios of APTES, respectively) were extracted with an ethanol:HCl (99:1) mixture, refluxed for 6 h and then filtered and dried in a vacuum oven at 55 °C for further 6 h.

Arsenate and Chromate-uptake studies

A stock solution of aqueous arsenate (1000 mg L^{-1}) was prepared by dissolving $Na_2HAsO_4.7H_2O$. Similarly, an aqueous solution of chromate stock solution (1000 mg L^{-1}) was prepared using K_2CrO_4. The prepared stock solutions were used for batch adsorption experiments. The pH of each test experiments were varied from 2 to 10 and solution pH were adjusted using 1 M sodium hydroxide or Nitric acid solution. The adsorption of Arsenate and Chromate by ICMS-N15 was investigated in a 50-mL glass vial. First, 25 mg of the ICMS-N is mixed with 25 mL of a stock metal ion solution (10–120 ppm). The adsorption process was conducted at 25 °C on an orbital shaker at a shaking speed of 150 rpm and the equilibrium constant (q_e) was determined using the following equation:

$$q_e = (C_i - C_e) \times (V / M)$$

where C_i is the initial concentration (mg L^{-1}), C_e is the equilibrium concentration (mg L^{-1}), V is the volume of the solution (L), and M is the mass of the adsorbent (g). The solutions were then filtered using a 0.45 mm filter paper and the arsenic/chromium concentration of the filtrate was analyzed by ICP-MS. We also analyzed the effect of ionic strength of common anions such as NO_3^-, Cl^-, PO_4^{3-} and SO_4^{2-} on the adsorption of arsenate and chromate. In this case, arsenate and chromate solutions with an initial concentration of 50 ppm were prepared and specific weight of sodium salt of aforementioned anions was added to make changes in ionic strength of test solution and test were conducted individually.

Characterization

Transmission electron microscopy (TEM) images were recorded on a JEOL 2010 electron microscope operating at 200 kV. The powder samples were dispersed in ethanol and then deposited and dried on a perforated Cu grid. The images were recorded at magnifications of 150,000× and 200,000×. Scanning electron microscopy (SEM) images were recorded on a JEOL JSM-6700F instrument. Small angle X-ray scattering (SAXS) was performed at the Pohang Accelerator Laboratory (PAL) with Co-Kα radiation (λ = 1.608 Å) in the energy range 4–16 keV (energy resolution: $\Delta E/E = 5 \times 10^{-4}$; photon flux: 10^{10}–10^{11} ph./s, beam size: <1 mm^2) over the scan range 0.1 nm^{-1} < q < 5.0 nm^{-1}. Nitrogen adsorption and desorption isotherms were measured using an ASAP 2020 surface area and pore size analyzer. Prior to the measurements, the samples were dehydrated at 95 °C for 6 h. The Brunauer–Emmett–Teller (BET) method was used to calculate the specific surface area. The pore size distribution was calculated from the isotherm desorption branch by the Barrett–Joyner–Halenda (BJH) method available with the apparatus software. The infrared spectra were recorded on a Nicolet 6700 FT-IR spectrometer. XPS analysis was performed using an X–ray photoelectron spectrometer (VG, ESCALAB 250) with monochromatic Al Kα radiation (hν = 1486.6 eV). The solid state 29Si CP/MAS NMR measurements were carried out on a Bruker ADVANCE II+ 400 MHz NMR system. Magic angle spinning was performed at a 6 kHz spinning rate and the contact time was fixed at 2 ms in all of the experiments. Elemental analyses were measured on a vario MICRO CHNS analysis technic.

Acknowledgements

This research work was supported by Basic Science Research Program through the National Research Foundation (NRF) of Korea (2012-0007172), BK21 PLUS through NRF (21A20131800002), and Korea government (MSIP) through GCRC-SOP (2011-0030013).

Notes and references

[a] *School of Chemical and Biomolecular Engineering, Pusan National University, Busan 609-735, Korea.*
[b] *Global Core Research Centre for Ships and Offshore Plants, Pusan National University, Busan 609 735, Korea*
*Corresponding author
E-mail: chems@pnu.edu
Tel.: +82 51 510 2397
Fax: +82 51 512 8563

† Electronic Supplementary Information (ESI) available: [details of any supplementary information available should be included here]. See DOI: 10.1039/b000000x/

References

1. R. S. Oremland and J. F. Stolz, *Science,* 2003, **300**, 939–944.
2. V. M. Boddu, K. Abburi, J. L. Talbott and E. D. Smith, *Environ. Sci. Technol*., 2003, **37**, 4449-4456.
3. R. Fukai, *Nature,* 1967, **213**, 901.
4. W. Gao, M. Majumder, L. B. Alemany, T. N. Narayanan, M. A. Ibarra, B. K. Pradhan and P. M. Ajayan, *ACS Appl. Mater. Interfaces,* 2011, **3**, 1821–1826.
5. F. D. Natalea, A. Ertoa, A. Lanciaa and D. Musmarra, *J. Hazard. Mater.,* 2011, **192**, 1842–1850.
6. S. Chiarle, M. Ratto and M. Rovatti, *Water research,* 2000, **34,** 2971–2978.
7. D. D. Shao, J. Hu and X. K. Wang, *Plasma Processes Polym*., 2010, **7**, 977–985.
8. R. Kala and T.P. Rao, *J. Sep. Sci*., 2006, **29**, 1281-1287.
9. J.T. Mayo, C. Yavuz, S. Yean, L. Cong, H. Shipley, W. Yu, J. Falkner, A. Kan, M. Tomson and V. L. Colvin, *Sci. Technol. Adv. Mater.,* 2007, **8,** 71–75.
10. A. Benhamou, J. P. Basly, M. Baudu, Z. Derriche and R. Hamacha, *Journal of Colloid and Interface Science,* 2013, **404**, 135-139.
11. H. Yoshitake, T. Yokoi and T. Tatsumi, *Chem. Mater*., 2002, **14**, 4603–4610.

12. J. Wang, X. Ma, G. Fang, X. Ye and S. Wang, *J. Hazard. Mater*., 2011, **186**, 1985-1992.
13. G.M. Ayoub, A. Hamzeh and L. Semerjian, *Desalination,* 2011, **273**, 359-365.
14. P. Xu, G.M. Zeng, D.L. Huang, G.X. Xie and Z.F. Liu, *Science of the Total Environment,* 2012, **424**, 1-10.
15. A. Z. M. Badruddoza, Z.B.Z. Shawon, M.T. Rahman, K. Hidajat and M. S. Uddin, *Chem. Eng. J*., 2013, **225**, 607-615.
16. B. Saha and C. Orvig, *Coordination Chemistry Reviews,* 2010, **254**, 2959–2972.
17. V. M. Boddu, K. Abburi, J. L. Talbott, E. D. Smith and R. Haasch, *Water Research,* 2008, **42**, 633-642.
18. Y.-T. Wei, Y.-M. Zheng and J. P. Chen, *Water Research,* 2011, **45**, 2290-2296.
19. Z. Li, J. C. Barnes, A. Bosoy, J. F. Stoddart and J. I. Zink, *Chem. Soc. Rev*., 2012, **41**, 2590-2605.
20. J. L. Vivero-Escoto, I. I. Slowing, B. G. Trewyn and V. S. Lin, *Small,* 2010, **6**, 1952-1967.
21. A. Walcarius, Chem. Soc. Rev., 2013, **42**, 4098-4140.
22. Y. Han and J. Y. Ying, *Angew. Chem. int. Ed*., 2005, **44**, 288–292.
23. T. W. Kim, P. W. Chung and V. S.-Y. Lin, *Chem. Mater*., 2010, **22**, 5093.
24. A. S. Maria and X. S. Zhao, *J. Phys. Chem. B*, 2003, **107**, 12650.
25. Sujandi, S.-E. Park, D.-S. Han, S.-C. Han, M.-J. Jin and T. Ohsuna., *Chem. Commun*., 2006, 4131–4133.
26. A. Singh, D. P. Dutta, J. Ramkumar, K. Bhattacharya, A. K. Tyagi and M. H. Fulekar, *RSC Adv*., 2013, **3**, 22580–22590.
27. W.-C. Huang, N.-C. Lai, L.-L. Chang, C.-M. Yang, *Microporous Mesoporous Mater*., 2012, **151**, 411–417.
28. S. Ravi, M. Selvaraj, *Dalton trans*. 2014, **43**, 5299-5308.
29. Z. Wu, D. Zhao, *Chem. Commun*. 2011, **47**, 3332–3338.
30. X. Chen, K. F. Lam and K. L. Yeung, *Chemical Engineering Journal*, 2011, **172**, 728–734.
31. N. Mahanta, J. P. Chen, *J. Mater. Chem. A* 2013, **1**, 8636-8644.
32. J. Lia, T. Qi , L. Wang, C. Liu and Y. Zhang, Materials Letters, 2007, 61, 3197–3200
33. H. Yoshitake, T. Yokoi and T. Tatsumi, *Chem. Lett*., 2002, 586–587.
34. K. F. Lam, K. L. Yeung and G. Mckay, *Microporous Mesoporous Mater*., 2007, **100**, 191–201.
35. S. V. Mattigod, G. E. Fryxell and K. E. Parker, *Inorg. Chem. Commun*., 2007, **10**, 646–648.
36. F. Mou, J. Guan, H. Ma, L. Xu, and W. Shi, *ACS Appl. Mater. Interfaces,* 2012, **4**, 3987–3993.
37. Yong Jia, T. Luo, X.-Y. Yu, B. Sun, J.-H. Liu and X.-J. Huang, *RSC Adv*., 2013, **3**, 5430–5437.
38. T. Wen, X. Wu, X. Tan, X. Wang, and A. Xu, *ACS Appl. Mater. Interfaces*, 2013, **5**, 3304–3311.
39. S. V. Mattigod, G. E. Fryxell and K. E. Parker, *Inorg. Chem. Commun*., 2007, **10**, 646–648.
40. V. Kailasam and E. Rosenberg, *Hydrometallurgy,* 2012, **129-130**, 97–104.
41. K. Sing, D. Everett, R. Haul, L. Moscou, R. Pierotti, J. Rouquerol,T. Siemieniewska, *Pure Appl. Chem*. 1985, **57**, 603–619.
42. X. Y. Bao and X. S. Zhao, J. Phys. Chem. B, 2005, **109**, 10727.
43. S. Deng, G. Yu, S. Xie, Y. Kuwaki, M. Iseki, *Langmuir* 2008, **24**, 10961-10967.
44. I. Langmuir, *J. Am. Chem. Soc*. 1918, **40**, 1361–1403.
45. M. P. Candela, J. M. Martinez, R. T. Macia, *Water Research* 1995, **29**, 2174–2180.
46. C. Han, H. Pu, H. Li, L. Deng, S. Huang, S. He and Y. Luo, *J. Hazard. Mater.,* 2013, **254**, 301–309.
47. H. Yoshitake, E. Koiso, H. Horie and H. Yoshimura, Microporous Mesoporous Mater., 2005, 85, 183–194.
48. E. McKimmy, J. Dulebohn, J. Shah and T. J. Pinnavaia, Chem. Commun., 2005, 3697–3699.
49. A. C. Zimmermann, A. Mecabo, T. Fagundes, C. A. Rodrigues, Journal of Hazardous Materials, 2010, 179, 192–196.